ELSEVIER

Thermochimica Acta 312 (1998) 17–25

thermochimica acta

Surface equilibration in adsorption microcalorimetry of bases on H-USY

S.M. Babitz[a], B.A. Williams[a], M.A. Kuehne[a], H.H Kung[a,*], Jeffrey T. Miller[b]

[a] *Department of Chemical Engineering, V.N. Ipatieff Laboratory, Northwestern University, 2145 Sheridan Road, Evanston, IL 60208-3120, USA*

[b] *Amoco Chemical Company, P.O. Box 3011, Mail Station E-1F, Naperville, IL 60566-7011, USA*

Abstract

It is commonly assumed that adsorbed basic probe molecules freely equilibrate with surface-acid sites in microcalorimetric experiments to determine the strength and distribution of the acid sites. The validity of this assumption was tested by comparing the differential heat of adsorption on H-USY as a function of surface coverage of CD_3NH_2, NH_3 and CD_3CN, which have widely different proton affinities, and by monitoring with FTIR the distribution of the adsorbed molecules between Brønsted- and Lewis-acid sites during adsorption and desorption. The results showed that full equilibration was achieved with the weakest base, CD_3CN, but not with the stronger bases, CD_3NH_2 or NH_3. © 1998 Elsevier Science B.V.

Keywords: Acid sites on HUSY; Adsorption of bases; Calorimetry; FTIR of adsorbed bases; HUSY acidity

1. Introduction

The acidic form of ultrastable Y zeolites (H-USY), prepared through steam dealumination of Y zeolites, are very effective solid–acid catalysts for the cracking of hydrocarbons. The activity enhancement from steaming is due to several changes in the structure of Y zeolite [1–4]. Some of these structural changes are thought to enhance the strength of acid sites in Y zeolite [5], and recent reviews show that much effort has been spent on trying to measure the number and strength of acid sites in these catalysts [6,7].

Effort to quantify the acid strength of solids has focused on techniques that measure the equilibrium between an adsorbed base molecule (B) and a surface-acid site (AH):

$$AH + B \rightleftharpoons A^- + BH^+ \quad (1)$$

An obstacle to accomplishing this task is the absence of knowledge to relate this equilibrium on a solid surface to the well-established equilibrium in an aqueous medium (pK_a). Application of the Hammett acidity function [8,9] (used with acids in non-aqueous solvents) to solid acids is inadequate for several reasons [10].

In particular, there are processes that occur in solution, such as the migration of ions and counter ions in order to achieve the most energetically favorable configuration and stabilization by solvent molecules, that are either impossible or different over a solid surface. In addition, there are experimental difficulties. Color changes using Hammett indicators may be difficult to follow on opaque or colored solids, other processes besides acid–base interactions can produce color changes (i.e. solvent–metal oxide interactions), and acid sites in micropores may be inaccessible to large indicator molecules.

Recently, adsorption microcalorimetry has become a popular technique for measuring acidity of solids [6,7]. In this technique, the differential heat of adsorp-

*Corresponding author.

PII S0040-6031(97)00436-X

tion (ΔH_{ads}) of a basic probe molecule is measured, and its magnitude is used as a measure of the strength of the acid site. By measuring the change in the heat of adsorption with coverage of the base molecule, the distribution of strengths of the acid sites can be obtained.

In order that this technique may yield an accurate representation of the acid-strength distribution, two important assumptions must be made: (1) The ΔH_{ads} is a property which is uniquely related to the strength of the acid sites; and (2) The adsorbed base is equilibrated among all the acid sites on the catalyst surface within the time frame of the experiment. Gorte et al. [11–15] have discussed the first assumption extensively and have questioned its validity. The problem arises from the fact that the ΔH_{ads} (reaction 1) is actually a sum of three reactions [14,15]:

$$AH_{(s)} + B_{(g)} \rightleftharpoons A^-_{(s)} + H^+_{(g)} + B_{(g)} \quad (2)$$

$$A^-_{(s)} + H^+_{(g)} + B_{(g)} \rightleftharpoons A^-_{(s)} + BH^+_{(g)} \quad (3)$$

$$A^-_{(s)} + BH^+_{(g)} \rightleftharpoons A^-_{(s)}BH^+_{(ad)} \quad (4)$$

The heat of reaction (2), the negative value of the proton affinity of the conjugate base of the acid site, is the desired quantity. However, this cannot be obtained from the ΔH_{ads} because the heat of reaction (4) is not known. (The heat of reaction (3) is the proton affinity of the base in the gas phase.) Thus, when the heats of adsorption for a given base over a series of catalysts are compared, in reality, both the strength of the acid sites (2) and the interaction energy of the protonated base with the surface conjugate base (4) are compared.

Concerns about the second assumption have been raised by various researchers [16–19]. It is recognized that the adsorption on surface sites could be controlled by kinetics instead of thermodynamics. In that case, the profile of ΔH_{ads}, as a function of coverage, would not accurately represent the distribution of acid strength. Dumesic et al. [18] have studied this issue of surface equilibration using both theoretical arguments and experimental data [19]. By using data from the heat of adsorption and the adsorption isotherm of pyridine on silica, Cardona-Martinez and Dumesic [18] estimated the entropy of adsorbed pyridine and the activation energy for its surface diffusion. They suggested that for a microcalorimetry experiment performed at 473 K, surface diffusion could be sufficient to permit equilibration of the probe molecule with surface sites.

To further test this conclusion, Spiewak et al. [19] compared the differential ΔH_{ads} measured by microcalorimetry and temperature programmed desorption (TPD) of ammonia at 423 K over γ-Al_2O_3 and HNa-Y zeolite. The comparison was found to be quite satisfactory. However, these results also indicated potential problems at low coverage of base where the ΔH_{ads} is high. They showed a sizable (30 kJ mol^{-1}) difference in the differential heats between the two measurements on HNa-Y at coverages below 100 μmol g^{-1}. This difference could potentially be greater over H-USY as this sample adsorbs NH_3 with ΔH_{ads} higher than HNa-Y (150 kJ mol^{-1} [20] vs. 130 kJ mol^{-1} [19]), and therefore surface diffusion may be more severely restricted. In our study of adsorption of methylamine, ammonia, and acetonitrile on H-USY, the initial calorimetric data suggested that equilibration of the probe base molecules with the surface sites was slower than first anticipated. This has led to a more detailed investigation to attempt to establish under what conditions equilibrium could be achieved, and here we report the results of this investigation.

Our investigation employed a combination of FTIR spectroscopy and microcalorimetry. FTIR spectra were collected after the H-USY sample was exposed to increasing doses of the probe base molecule, and during stepwise desorption from saturation coverage. Comparison of the spectra of comparable surface coverages in these two cases would allow us to quantitatively determine whether the acid sites were populated during adsorption and vacated during desorption in exactly opposite sequence; which must be the case if the adsorbed base has reached equilibrium among the acid sites on the sample.

2. Experimental

2.1. Catalyst preparation and physical characterization

The H-USY sample was prepared from NH_4-USY (UOP, LZ-Y84) by calcining in air at 723 K for 16 h. The sample crystallinity and unit cell constant were obtained by powder XRD. Adsorption of N_2 was used to determine the micropore volume and surface area.

Table 1
H-USY physical characterization

Property	Value
% XRD [a]	94
a_0 (Å)	24.468
Al_F/u.c.	26
Al_{Oct}/u.c.	18
Pore vol [b] ($cm^3\ g^{-1}$)	0.252
Pore S.A. [b] ($m^2\ g^{-1}$)	550
Na content (mmol g^{-1})	0.05

[a] This value is referenced against Na-Y, UOP-LZY-52.
[b] Both the pore volume and surface area refer to micropore volume and surface area.

The Na content was determined by AA-ICP. The number of framework Al atoms per unit cell (Al_F/u.c.) was obtained, using the correlation developed, by Fichtner-Schmittler et al. [21] for steam dealuminated zeolites:

$$Al_F/\text{u.c.} = 112.4(a_0 - 24.233) \quad (5)$$

^{27}Al-MASNMR was used to determine the number of octahedral aluminum per unit cell (Al_{Oct}/u.c.) [22]. The physical properties of the H-USY are summarized in Table 1.

2.2. Adsorption microcalorimetry

The H-USY was pressed into a large wafer at 39 MPa (5700 psi) and was broken into 20/40 mesh pieces. A home made Tian–Calvet calorimeter was used to collect data for adsorption of NH_3 and CD_3NH_2 on H-USY. For these experiments, ca. 0.2–0.3 g of zeolite was used. Data for CD_3CN adsorption was collected prior to the construction of this calorimeter, and these data were collected using a Setaram DSC-111 with ca. 0.07–0.1 g of zeolite. The reference cells for both calorimeters contained an equal volume of 25/45 mesh quartz chips. The samples were pretreated in vacuo at 573 K for 16 h. They were then cooled to 473 K for experiments using NH_3 and CD_3NH_2. A lower temperature, 373 K, was necessary for experiments with CD_3CN, as it does not bind to the zeolite surface as strongly and was found to decompose on the zeolite surface at higher temperatures.

Sequential doses of ca. 6 μmol of base were admitted to the sample cell, while the heat evolved for each dose was monitored with the calorimeter. Heat evolution for each dose was assumed complete when the calorimeter output returned to the baseline value recorded prior to the dose. This took over 2 h for the early doses and ca. 20 min for the final doses. Data were collected until the pressure in the calorimetry cell was rising at a large, approximately constant rate with increasing coverage. The coverage at which this occurred was different for each of the bases. It should be emphasized that the use of two different calorimeters in this study should not affect interpretation of the data. Experiments performed with adsorption of CD_3CN on a ZSM-5 sample (Conteka, CBV-5020) showed that the two calorimeters gave nearly identical results.

2.3. FTIR

FTIR data were collected using a Mattson Galaxy 5022 spectrometer. The zeolite powder was pressed at 190 MPa (28 000 psi) to make a thin wafer weighing ≈10 mg cm^{-2}. The wafer was mounted in the transmittance IR cell in the center of a 3-in long heated zone; then treated in vacuo at 573 K for 16 h, and thereafter cooled to 473 K for experiments with NH_3 and CD_3NH_2 and to 373 K for experiments with CD_3CN. Doses of base molecules (ca. 6 μmol doses) were admitted into the cell, and after allowing the dose to equilibrate with the sample for a period of time comparable to that in the calorimetry experiments, a spectrum was collected. Desorption from the wafer after saturation coverage was achieved in a stepwise fashion by evacuating the cell for a brief period of time at elevated temperatures. In the case of CD_3CN, only evacuation was sufficient for desorption. The sample was allowed to equilibrate for about the same time as during adsorption, before a spectrum was collected at the same temperature as during the adsorption.

In most cases, the spectra shown are referenced to a fresh H-USY sample. Accordingly, adsorption of base onto the zeolite will appear spectroscopically as positive peaks for the adsorbed base in the N–H bending and C–N stretching regions and negative peaks in the hydroxyl stretching region. In all cases except where noted, each spectrum was collected with 1024 scans at a resolution of 2.0 or 4.0 cm^{-1}.

3. Results

3.1. Microcalorimetry

The data for the ΔH_{ads} as a function of coverage for CD_3NH_2, NH_3, and CD_3CN on H-USY are presented in Fig. 1. Among the three bases, CD_3NH_2 produced the highest heats of adsorption of ca. 150 kJ mol^{-1} up to a coverage of 650 μmol g^{-1}. The heat then decreased almost linearly with coverage to 100 kJ mol^{-1} at a coverage of 1350 μmol g^{-1}. NH_3 exhibited high initial heats of 140–150 kJ mol^{-1} below 100 μmol g^{-1}, and then lower heats with increasing coverage to ca. 95 kJ mol^{-1} at 1350 μmol g^{-1}. CD_3CN exhibited a much lower heat of adsorption than the other two bases. Initial ΔH_{ads} with CD_3CN was 110–120 kJ mol^{-1}, and then decreased to 70 kJ mol^{-1} at 1200 μmol g^{-1}.

The profiles of the differential ΔH_{ads} curves for the three bases are compared in Fig. 2. For clarity, the differential ΔH_{ads} values were normalized. The figure shows that the profiles were different for the three bases. For CD_3NH_2, it was relatively flat up to a coverage of 650 μmol g^{-1} before decreasing with increasing coverage. For both NH_3 and CD_3CN, it showed a decrease over the entire coverage range measured, but the rate of this decrease was greater for CD_3CN.

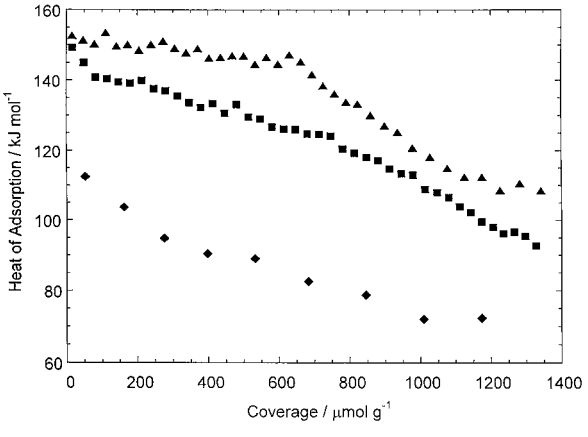

Fig. 1. Differential ΔH_{ads} of CD_3NH_2 at 200°C (▲), NH_3 at 200°C (■) and CD_3CN at 100°C (◆) on H-USY.

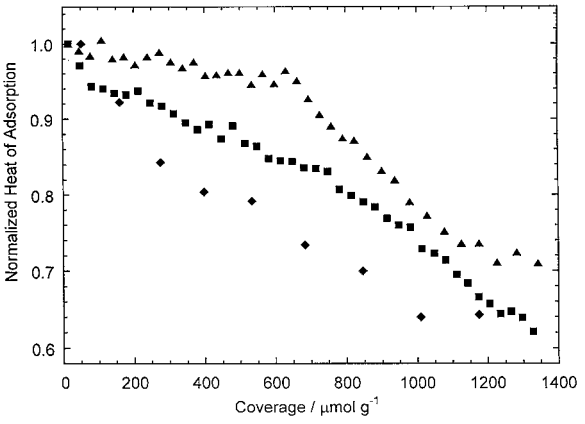

Fig. 2. Normalized differential ΔH_{ads} (normalized to the initial ΔH_{ads}) for CD_3NH_2 at 200°C (▲), NH_3 at 200°C (■) and CD_3CN at 100°C (◆) on H-USY.

3.2. FTIR spectroscopy

3.2.1. Methylamine

Spectra for CD_3NH_2 adsorption are presented in Figs. 3–5. The band assignments were made with spectra of CD_3NH_2 adsorbed on HY and γ-Al_2O_3 at 473 K. The HY was prepared by in situ calcination of NH_4Y, and ^{27}Al-MASNMR indicated that the majority of the aluminum in this sample was in the zeolite framework (85% of the aluminum is in tetrahedral coordination) [22]. The spectrum of CD_3NH_2 on HY

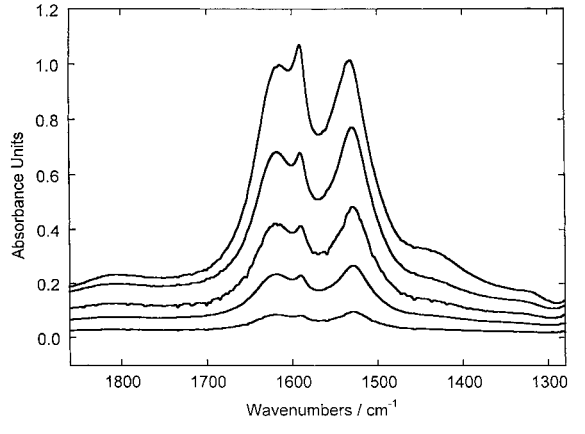

Fig. 3. N–H bending region of FTIR spectra taken at 200°C after CD_3NH_2 adsorption on H-USY. Coverages for selected doses (beginning with the bottom spectra) are 90, 260, 450, 670, and 1200 μmol g^{-1}.

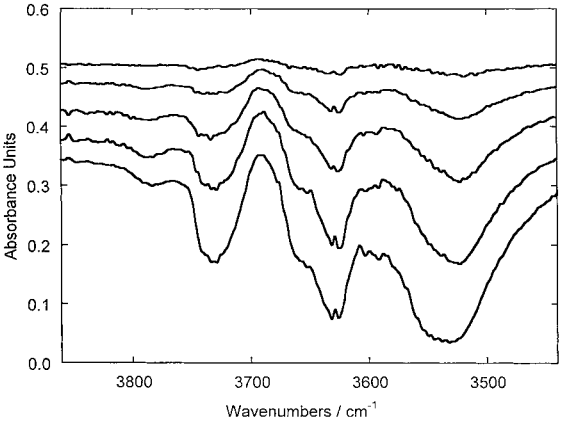

Fig. 4. O–H stretching region of FTIR spectra taken at 200°C after CD_3NH_2 adsorption on H-USY. Coverages for selected doses (beginning with the top spectra) are 90, 260, 450, 670, and 1200 μmol g^{-1}.

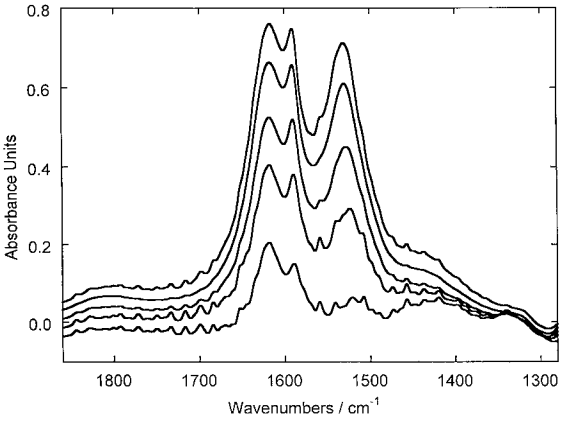

Fig. 5. N–H bending region of FTIR spectra taken at 200°C after CD_3NH_2 desorption from saturation coverage (beginning with the top spectra) at 250, 300, 350, 400, and 450°C on H-USY. Coverages (beginning with the top spectra) are 970, 880, 770, 670, and 450 μmol g^{-1}.

yielded bands at ≈1530 and 1620 cm^{-1}. They are assigned to symmetric and asymmetric N–H bending modes for adsorbed CD_3NH_2 on Brønsted-acid sites, respectively. Adsorption of CD_3NH_2 on γ-Al_2O_3 (Johnson Matthey, 99.97% purity) produced an N–H bending mode ca. 1595 cm^{-1}, which was assigned to NH_2 bending of adsorbed CD_3NH_2 on a Lewis-acid site. These band assignments are consistent with those determined by Ghosh and Curthoys [23] for methylamine adsorbed on a Y-type zeolite.

Fig. 3 shows the spectra in the N–H bending region at different CD_3NH_2 surface coverages during the adsorption cycle. The peaks at 1530, 1620, and 1595 cm^{-1} all increased proportionally with increasing coverage. The changes in the hydroxyl region for these same adsorption spectra are shown in Fig. 4. The bands for adsorption on terminal silanols (3740 cm^{-1}), HF hydroxyl groups in the supercages (3630 cm^{-1}), and LF hydroxyls in the sodalite cages (3530–3550 cm^{-1}) decreased roughly proportionally with increasing coverage [24–26]. Fig. 5 shows the spectra during the desorption cycle. After each desorption step, the temperature was lowered to 473 K to record a spectrum. These spectra showed that the bands for CD_3NH_2 on Brønsted-acid sites decreased faster than the band for adsorption on Lewis-acid sites. Thus, at low coverages, a higher percentage of the CD_3NH_2 was on Lewis-acid sites during desorption than during adsorption.

3.2.2. Ammonia

Spectra for NH_3 adsorption are presented in Figs. 6–8. Ammonia adsorption produced a peak at 1440 cm^{-1} due to adsorption on Brønsted-acid sites, and peaks at 1625 and 1316 cm^{-1} due to adsorption on Lewis-acid sites [27].

Fig. 6 shows the N–H bending region for ammonia adsorption on H-USY at 473 K. It shows a large peak

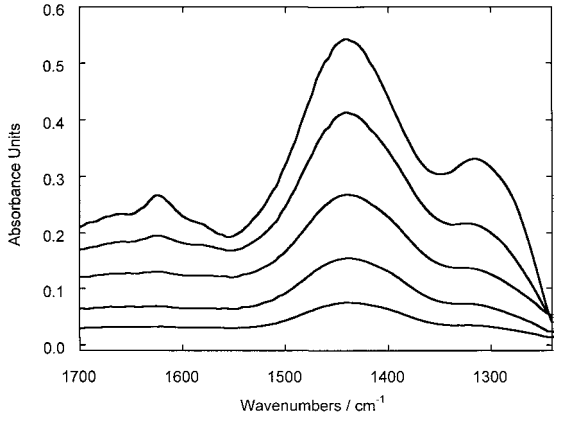

Fig. 6. N–H bending region of FTIR spectra taken at 200°C after NH_3 adsorption on H-USY. Coverages for selected doses (beginning with the bottom spectra) are 100, 200, 300, 630, and 1500 μmol g^{-1}.

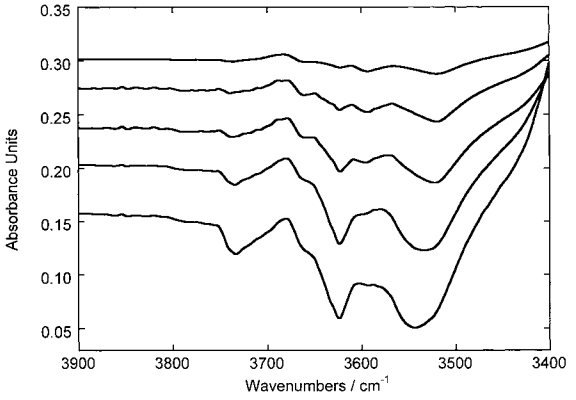

Fig. 7. O–H stretching region of FTIR spectra taken at 200°C after NH_3 adsorption on H-USY. Coverages for selected doses (beginning with the top spectra) are 100, 200, 300, 630 and 1500 μmol g^{-1}.

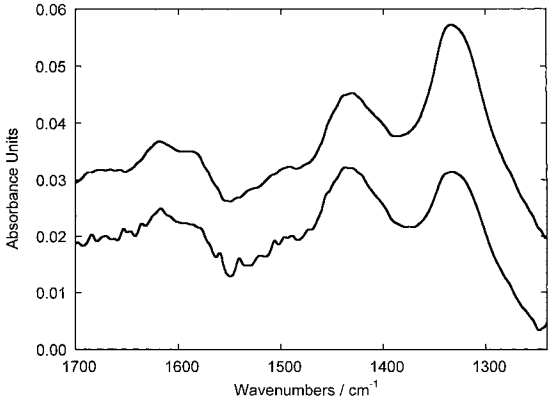

Fig. 8. N–H bending region of FTIR spectra taken at 200°C after NH_3 desorption from saturation coverage (beginning with the bottom spectra) at 350 and 300°C on H-USY. Coverages are less than 100 μmol g^{-1}.

for adsorption on Brønsted-acid sites, and two smaller peaks for adsorption on Lewis sites. Fig. 7 shows the corresponding spectra for the O–H stretching region. Similar to the changes in the adsorption of methylamine, decreases in the intensity of the bands for the terminal SiOH (3740 cm^{-1}), the Brønsted hydroxyl groups in the zeolite supercages (HF band at 3630 cm^{-1}), and the hydroxyl groups in the sodalite cages (LF band ca. 3530–3550 cm^{-1}) were observed. In addition, a small band ca. 3600 cm^{-1} could be detected at low NH_3 coverages, but became less pronounced at higher coverages.

After saturation coverage, the sample was heated in vacuum at 573 K for 8 h. After cooling the sample down to 473 K, a spectrum was recorded. The sample was then heated to 623 K for 30 min in vacuum and, subsequently, cooled to 473 K to take another spectrum. These spectra are shown in Fig. 8. A comparison of these two spectra with those in the adsorption cycle (Fig. 6) showed that the peaks for adsorption on Brønsted-acid sites were much more intense relative to the Lewis-acid peaks during the adsorption cycle. In contrast, despite the much lower adsorption coefficient [20], the Lewis-acid peak intensities were much greater than the Brønsted-acid peaks in the desorption spectra.

3.2.3. Acetonitrile

FTIR spectra for CD_3CN adsorption are shown in Figs. 9–11. The C–N stretch of CD_3CN adsorbed on a Lewis-acid site produced a peak at ca. 2320 cm^{-1}. For adsorption on a Brønsted-acid site, this mode appeared at 2296 and 2275 cm^{-1} for adsorption on a silanol group. In addition, an asymmetric CD stretch at 2250 cm^{-1} and a CD symmetric stretching band at 2111 cm^{-1} were also observed [28].

The spectra for CD_3CN adsorption (Fig. 9) and desorption (Fig. 10) were similar to one another. At low coverages, only the Lewis-acid peak was observed (in addition to the CD stretches). As the coverage increased, peaks corresponding to adsorption on

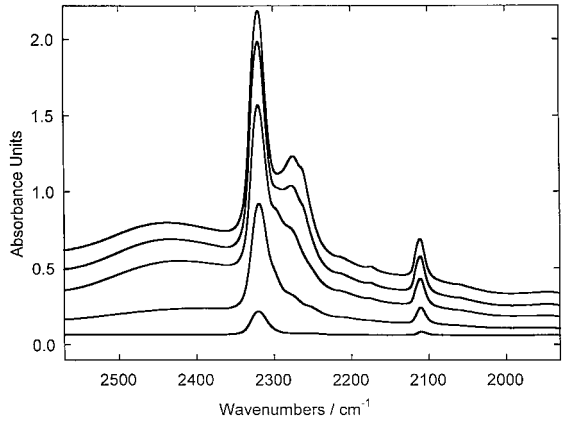

Fig. 9. C–N stretching region of FTIR spectra taken at 100°C after CD_3CN adsorption on H-USY. Coverages for selected doses (beginning with the bottom spectra) are 70, 350, 850, 1350, and 1580 μmol g^{-1}.

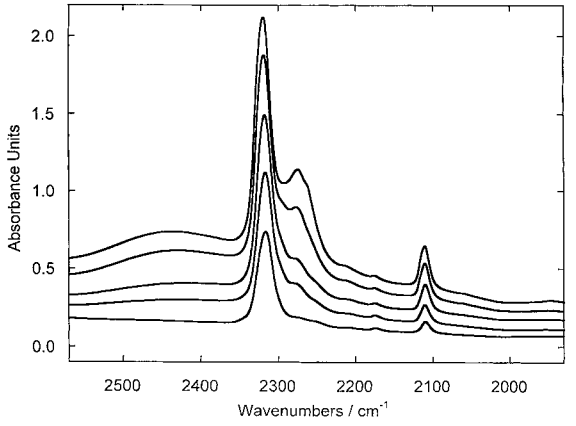

Fig. 10. C–N stretching region of FTIR spectra taken at 100°C after CD_3CN desorption from saturation coverage on H-USY. Coverages for selected doses (beginning with bottom spectra) are 170, 350, 800, 1130, and 1500 μmol g^{-1}.

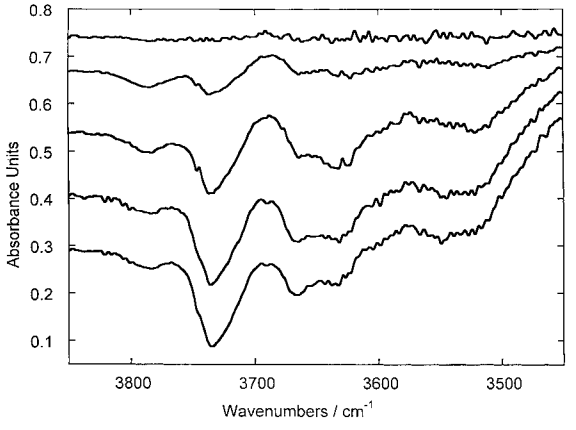

Fig. 11. O–H stretching region of FTIR spectra taken at 100°C after CD_3CN adsorption on H-USY. Coverages for selected doses (beginning with the bottom spectra) are 1580, 1350, 850, 350, and 70 μmol g^{-1}.

Brønsted and silanol sites appeared as shoulders to the Lewis-acid peak. In addition, the Lewis-acid peak shifted slightly to a lower frequency at higher coverage. This indicated a weaker interaction of CD_3CN with the Lewis-acid site; implying that weaker Lewis-acid sites were populated at higher coverages.

The spectra of the hydroxyl region during CD_3CN adsorption showed increasing perturbation of the HF, LF and silanol hydroxyls with increasing coverage after the first few doses of CD_3CN. Unlike the corresponding spectra for NH_3 and CD_3NH_2 adsorption, the decrease in the intensity of the silanol peak (3735 cm^{-1}) was much more pronounced for CD_3CN, whereas the decrease in the LF peak was much less.

4. Discussion

Microcalorimetry has been used as a standard method to characterize solid acids in the last two decades. One extremely useful piece of information that microcalorimetry provides, much more readily than other techniques, is the distribution of acid-site strengths. As mentioned in Section 1, in order for the microcalorimetry data to accurately reflect this distribution, it is assumed that the adsorbed base molecules are fully equilibrated with the surface sites such that these sites are occupied sequentially according to their acid strengths; allowing for entropic effects at elevated temperatures.

In the literature, pyridine and NH_3 are the most commonly used base probe molecules for characterizing solid acids. These two molecules are rather basic, with gas-phase proton affinities of 924.0 and 853.5 kJ mol^{-1}, respectively [29]. The initial ΔH_{ads} for these two molecules on H-USY follow the same order [20,30], being 250 and 150 kJ mol^{-1}, respectively.

In this study, the ΔH_{ads} profiles were obtained for CD_3NH_2, NH_3 and CD_3CN. Since the proton affinities of these molecules are quite different (gas-phase proton affinities are 896.0, 853.5, and 788.0 kJ mol^{-1}, respectively [29]), their ΔH_{ads} profiles could provide a rather sensitive test on the assumption of surface equilibration. That is, if adsorption of these molecules are fully equilibrated and the ΔH_{ads} profiles accurately reflect the strength distribution of the acid sites, then the profiles of the three molecules should be identical. This is clearly not the case as shown by Figs. 1 and 2.

There are two possible reasons for the different profiles. Either the adsorption of some or all of the molecules is not fully equilibrated, or the interaction of the surface conjugated base with the protonated probe molecule is different (reaction (4)). Unfortunately there is no direct experimental information available on the latter quantity. On the other hand, the FTIR data provide information on equilibration of

the adsorbed base molecules among sites on the zeolite surface. Since the FTIR spectra provide quantitative information on the number of molecules adsorbed on the Brønsted- and Lewis-acid sites, it is possible to determine the distribution of the adsorbed molecules between these sites as a function of coverage. In the case of CD_3NH_2 and CD_3CN, the symmetric C–D stretching peak at ca. 2100 cm^{-1} can be used to quantitatively compare surface coverages in different spectra. It is expected that, if adsorption is fully equilibrated, the distribution of adsorbed molecules between Brønsted- and Lewis-acid sites will be identical at the same surface coverage for both the adsorption and desorption processes, since it should be a thermodynamic state quantity, independent of the process to achieve that state. This is observed for adsorption of CD_3CN. Figs. 9 and 10 show identical distributions on different sites for the same CD_3CN coverage. On the other hand, adsorption equilibration is not achieved with CD_3NH_2 or NH_3, since the FTIR spectra for the adsorption and desorption processes are different (Figs. 3, 5, 6 and 8).

Achieving equilibration for CD_3CN and not for CD_3NH_2 or NH_3 is consistent with the fact that CD_3CN is the weakest of the three bases. Not only is its gas-phase proton affinity lower, its ΔH_{ads} is substantially lower. Since the heat of adsorption is a direct measure of the strength of the interaction of the molecule with the surface, which in turn is related to the activation energy for surface diffusion, it is expected that the adsorption of CD_3NH_2 would be the furthest from full equilibration.

If adsorption of a probe molecule is so strong that there is no surface diffusion at all, then the probe molecule would not be able to distinguish among surface sites of different adsorption strengths. In this case, the adsorption is kinetically controlled, and the ΔH_{ads} profile would reflect the relative rates of adsorption on various sites; sites that adsorb molecules faster are measured first [16,17]. If adsorption on all these sites occurs at the same rate, then the probe molecule would adsorb on the first unoccupied site it encounters, and the resulting ΔH_{ads} profile for a sample of spatially and randomly distributed sites could be a curve of constant heat up until full surface coverage. While no measurements were made here of the adsorption kinetics, the relatively constant ΔH_{ads} observed for CD_3NH_2 suggests that this molecule

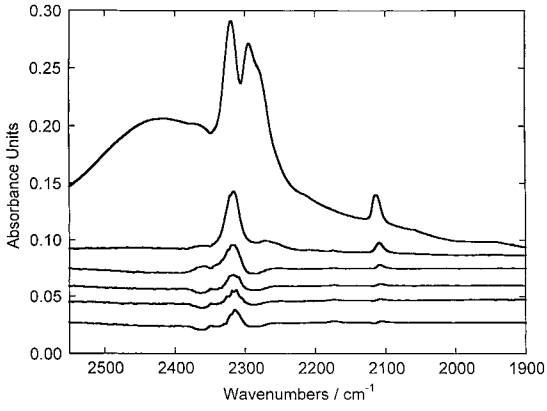

Fig. 12. Time evolution of the C–N stretching region during CD_3CN adsorption at ca. 500 μmol g^{-1}. Each spectra was collected with 256 scans taken at (beginning with the top spectra) 5, 15, 25, 35, 45, and 60 min after introduction of the dose. The background for each spectra is the preceding. All spectra (except 5 min) were multiplied by a factor of 2.0 for display purposes.

adsorbs statistically and with little surface diffusion. The profiles for NH_3 and CD_3CN show more distinction among different sites (Figs. 1 and 2). Thus, as concluded earlier, the adsorption of CD_3NH_2 and NH_3 are not fully equilibrated.

In fact, even for the weak base CD_3CN, equilibration was not instantaneous. As shown in Fig. 12, CD_3CN first adsorbs on both Brønsted (2296 cm^{-1})- and Lewis (2320 cm^{-1})-acid sites. When the system was allowed to evolve with time, migration of adsorbed molecules from the Brønsted- to Lewis-acid sites occurs. Equilibration is achieved within an hour under these conditions. With such slow equilibration for a weakly adsorbed molecule, it is not surprising that equilibration is not achieved with CD_3NH_2 or NH_3.

5. Conclusions

It is established in this study that the assumption of equilibration of adsorbed molecules with surface-acid sites in microcalorimetric experiments is confirmed for weak bases on H-USY, such as acetonitrile with ΔH_{ads} of 110–120 kJ mol^{-1}. For stronger bases, such as NH_3 and CD_3NH_2 with ΔH_{ads} of 150 kJ mol^{-1} or higher, equilibration is not achieved within the time scale of the experiment. That is, equilibration is not

achieved in up to 2 h. Consequently, the ΔH_{ads} profiles for these molecules do not accurately reflect the acid-strength distribution on the solid. These results show that equilibration is achieved only with much weaker bases than previously assumed.

Acknowledgements

Financial support of this work by the National Science Foundation and in kind support by Amoco Corporation are gratefully acknowledged.

References

[1] C. Choi-Feng, J.B. Hall, B.J. Huggins, R.A. Beyerlein, J. Catal. 140 (1993) 395.
[2] R.A. Beyerlein, G.A. Tamborski, C.L. Marshall, B.L. Meyers, J.B. Hall, B.J. Huggins, in: M.L. Occelli (Ed.), Fluid Catalytic Cracking II, ACS Symposium Series 452, American Chemical Society, Washington, DC, 1991, pp. 109–143.
[3] P. Gélin, T.Des Courières, Appl. Catal. 72 (1991) 179.
[4] P. Fejes, I. Kiricsi, I. Hannus, Gy. Schöbel, in: D. Kallò, Kh.M. Minachev (Eds.), Catalysis on Zeolites, Akadémiai Kiadò, Budapest (distribtued by H. Stillman: Boca Raton, FL), 1988, pp. 205–229.
[5] J.H. Lunsford, in: M.L. Occelli (Ed.), Fluid Catalytic Cracking II, ACS Symposium Series 452; American Chemical Society, Washington, DC, 1991, pp. 1–11.
[6] N. Cardona-Martinez, J.A. Dumesic, Adv. Catal. 38 (1992) 149.
[7] P.J. Andersen, H.H. Kung, Catalysis 11 (1994) 441.
[8] L.P. Hammett, A.J. Deyrup, J. Am. Chem. Soc. 54 (1932) 2721.
[9] C. Rochester, Acidity Functions, Organic Chemistry Series, vol. 17, Academic press, New York, 1970.
[10] D. Farcasiu, A. Ghenciu, G. Miller, J. Catal. 134 (1992) 118.
[11] M.T. Aronson, R.J. Gorte, W.E. Farneth, J. Catal. 98 (1986) 434.
[12] D.J. Parillo, R.J. Gorte, Catt. Lett. 16 (1992) 17.
[13] D.J. Parillo, R.J. Gorte, J. Phys. Chem. 97 (1993) 8786.
[14] D.J. Parillo, C. Lee, R.J. Gorte, D. White, W.E. Farneth, J. Phys. Chem. 99 (1995) 9745.
[15] W.E. Farneth, R.J. Gorte, Chem. Rev. 95 (1995) 615.
[16] G. Ehrlich, J. Chem. Phys. 36 (1962) 1171.
[17] M. O'Neil, J. Phillips, J. Phys. Chem. 91 (1987) 2867.
[18] N. Cardona-Martinez, J.A. Dumesic, J. Catal. 125 (1990) 427.
[19] B.E. Spiewak, B.E. Handy, S.B. Sharma, J.A. Dumesic, Catt. Lett. 23 (1994) 207.
[20] M.A. Kuehne, H.H. Kung, J.T. Miller, submitted to J. Catal., 1997.
[21] H. Fichtner-Schmittler, U. Lohse, G. Engelhardt, V. Patzelová, Cryst. Res. Technol. 19 (1984) K1.
[22] D.C. Koningsberger, J.T. Miller, in: J.W. Hightower, W.N. Delgass, E. Iglesia, A.T. Bell (Eds.), 11th International Congress on Catalysis – 40th Anniversary, Studies in Surface Science and Catalysis, vol. 101-B, Elsevier: Amsterdam, 1996, pp. 841–850.
[23] A.K. Ghosh, G. Curthoys, J. Chem. Soc. Faraday Trans. I 80 (1984) 99.
[24] J.W. Ward, J. Catal. 19 (1970) 248.
[25] P.A. Jacobs, J.B. Uytterhoeven, J. Chem. Soc. Faraday Trans. I. 69 (1973) 359.
[26] G. Garralon, A. Corma, V. Fornes, Zeolites 9 (1989) 84.
[27] H. Kosslick, H. Berndt, H.D. Lanh, A. Martin, H. Miessner, V.A. Tuan, J. Jänchen, J. Chem. Soc., Faraday Trans. 90 (1984) 2837.
[28] A.G. Pelmenschikov, R.A. van Santen, J. Jänchen, E. Meijer, J. Phys. Chem. 97 (1993) 11071.
[29] S.G. Lias, J.F. Liebman, R.D. Levin, J. Phys. Chem. Ref. Data 13 (1984) 695.
[30] D.T. Chen, S.B. Sharma, I. Filimonov, J.A. Dumesic, Catt. Lett. 12 (1992) 201.